LbL Fabricated Poly(Styrene Sulfonate)/TiO$_2$ Multilayer Thin Films for Environmental Applications

D. Neela Priya,[†] Jayant M. Modak,[‡] and Ashok M. Raichur*,[†]

Departments of Materials Engineering and Chemical Engineering, Indian Institute of Science, Bangalore, 560012, India

ABSTRACT Fabrication of multilayer ultrathin composite films composed of nanosized titanium dioxide particles (P25, Degussa) and polyelectrolytes (PELs), such as poly(allyl amine hydrochloride) (PAH) and poly(styrene sulfonate sodium salt) (PSS), on glass substrates using the layer-by-layer (LbL) assembly technique and its potential application for the photodegradation of rhodamine B under ultraviolet (UV) irradiation has been reported. The polyelectrolytes and TiO$_2$ were deposited on glass substrates at pH 2.5 and the growth of the multilayers was studied using UV/vis spectrophotometer. Thickness measurements of the films showed a linear increase in film thickness with increase in number of bilayers. The surface microstructure of the thin films was characterized by field emission scanning electron microscope. The ability of the catalysts immobilized by this technique was compared with TiO$_2$ films prepared by drop casting and spin coating methods. Comparison has been made in terms of film stability and photodegradation of rhodamine B. Process variables such as the effect of surface area of the multilayers, number of bilayers, and initial dye concentration on photodegradation of rhodamine B were studied. Degradation efficiency increased with increase in number of catalysts (total surface area) and bilayers. Kinetics analysis indicated that the photodegradation rates follow first order kinetics. Under maximum loading of TiO$_2$, with five catalyst slides having 20 bilayers of polyelectrolyte/TiO$_2$ on each, 100 mL of 10 mg/L dye solution could be degraded completely in 4 h. The same slides could be reused with the same efficiency for several cycles. This study demonstrates that nanoparticles can be used in wastewater treatment using a simple immobilization technique. This makes the process an attractive option for scale up.

KEYWORDS: layer-by-layer method • multilayer thin films • titanium dioxide • photodegradation • rhodamine B

INTRODUCTION

Industrial development is directly related to the disposal of various toxic pollutants mainly in to the aqueous streams, that are harmful to the environment and hazardous to human health. The pollutants in water include heavy metals, inorganic and organic contaminants; however, the biggest concern is the presence of various types of organic contaminants that are not adequately removed by conventional water treatment technologies. Therefore, new approaches and improved advanced technologies need to be developed, to effectively address these water quality challenges and to completely degrade the organic contaminants. Application of nanoparticles in water treatment is an emerging area and nanocatalysts have proven to have a potential to treat organic contaminants and play an important role in solving many serious environmental and pollution challenges (1).

Heterogeneous photocatalysis using semiconductor materials like TiO$_2$ (2), ZnO (3), Fe$_2$O$_3$ (4), CdS (5), and ZnS (6) appears as a promising advanced oxidation technology leading to the total mineralization of most of organics.

Among the available catalysts, TiO$_2$ finds wider application because of its availability, stability, low cost, and favorable band gap energy (7). Researchers have studied different kinds of TiO$_2$, such as the combustion-synthesized TiO$_2$ and Degussa P25 for the photocatalytic degradation of various organics (8−12). Although the use of suspended TiO$_2$ powder is efficient because of the large surface area of catalyst available for reaction, it has several disadvantages like the catalyst cannot be recovered and reused efficiently for continuous systems which would directly incur high treatment costs making such process economically unviable (13, 14).

Because of these problems, there has been an increasing interest in the fabrication of thin films. These films can be fabricated by methods such as, sol−gel synthesis, sputtering, chemical vapor deposition (CVD), spray pyrolysis, ion-assisted deposition, arc ion plating, dip coating, drop casting, and spin coating (15−22). But these methods have some drawbacks like high temperature requirement (in CVD) and difficulty in controlling the thickness (in sol−gel process). Decher and Hong (23) reported a novel thin film making method called the layer-by-layer (LbL) assembly multilayer technique which can be used to deposit various types of materials on different kind of substrates. Among several methods, this method provides a simple way to immobilize highly accessible, well-separated nanoparticles in porous membranes and afford control over the amount of material deposited. The method is based on the electrostatic attrac-

tion between oppositely charged polyelectrolytes or inorganic charged species, such as metal colloids (24) or nanoparticles (25) of semiconductors, or metal oxides, such as TiO_2 (26, 27).

Over the past few decades, the polyelectrolyte materials have emerged as a new class of materials that can be tailor-made to suit various applications, such as antireflective coatings (28), biosensing (29), controlled drug delivery (30), and for use in materials (31). Attempts have also been made to coat TiO_2 on polymer films which have proven to be beneficial in improving the photocatalytic performances (32). Kim and Sohn (33, 34) studied the morphology and photocatalytic activity of LBL-SA PAH/PAA/TiO_2 films and their application for photooxidation of iodide ions and decomposition of methyl orange. They further extended the work to compare the photocatalytic activity of these films prepared by dip SA and spin SA and showed how the fabrication process of films using different constructing materials affects the physical and photocatalytic properties.

Among the different organic pollutants of aquatic ecosystems, dyes constitute a large and important group of industrial chemicals. Rhodamine B, one of the most important dyes of the xanthene group is used in many industrial processes, such as paper dyeing and production of dye laser (15). In the present study, rhodamine B dye was selected as a representative pollutant due to its wide application range and recalcitrant nature. Photodegradation of rhodamine B using TiO_2 immobilized on different supports and different methods have been studied earlier by many researchers (14, 35−38). However, application of LbL technique and the polyelectrolyte system used for immobilization of catalysts in the present study for the photodegradation of Rhodamine B has not been reported until date.

In this paper, we demonstrate the utility of LbL technique to fabricate PSS/TiO_2 multilayer thin films and its application for photocatalytic degradation of Rhodamine B. This would alleviate all the drawbacks associated with TiO_2 used earlier in powder and suspension form. Unlike the systems that used weak polyelectrolytes (33) for fabrication of thin films, in the present study, a strong polyelectrolyte, such as PSS, is used for assembling, which is negatively charged at all pH values. The advantage of using such PSS/TiO_2 films in terms of its ordered nonporous structure (27) and the relative hardness (39) of such films has been reported by researchers. In addition, the LbL method has been compared with other methods, such as spin-coating and drop-casting methods, to show its effectiveness in terms of film morphology and dye degradation. In light of the hazardous nature and harmful effects of the dye, it was considered worthwhile to make systematic efforts to completely degrade it from wastewaters using this technique. In our research, we are mainly looking at cost-effective and sustainable way of removing and completely degrading the dye from wastewaters. Hence, catalyst reusability studies have also been performed to show that the method employed is very significant from both economic and environmental perspectives.

EXPERIMENTAL SECTION

Materials. Poly(styrene sulfonate sodium salt) (PSS, M_W = 70 000 g/mol) and poly(allylamine hydrochloride) (PAH, M_W = 70 000 g/mol) used for film preparation were obtained from Sigma-Aldrich (USA). Rhodamine B dye was obtained from SD Fine Chemicals India Ltd. (Mumbai) and was used as reactant in photodegradation reactions. Commercial TiO_2 powder Aeroxide P25 (average particle size: 21 nm, Degussa AG, Germany), which contains about 80 % of anatase and 20 % of rutile with a BET specific surface area of about 50 m²/g was used as received. Microscopic glass slides (25.4 × 63.5 mm) were used as substrates. Millipore water (18 MΩ resistivity) was used for rinsing/washing films. For pH adjustments, 1 M HCl/NaOH solutions prepared in DI water were used.

Apparatus. A digital pH meter (Model Orion 5 star, Thermo Electron Corporation, USA) was used for adjusting the pH of the solutions. Absorbance spectra of the polyelectrolyte layers were obtained using UV/vis spectrophotometer (T60U Spectrophotometer, PG Instruments Ltd., UK). The thickness of the films was measured on a nonconatct optical profilometer (Wyco NT 1100 Optical profiling System, Veeco instruments, USA). The effectiveness of the multilayer films was verified using atomic force microscope (MF3D AFM, Asylum Research, USA). The surface morphology of the thin films was examined using a field emission scanning electron microscope (FEI-SIRION, Eindhoven, The Netherlands). Spin coating experiments were performed on a spin coater.

Photocatalytic Reactor. The photoreactor consists of a jacketed quartz tube with dimensions of 3.4 cm inner diameter, 4 cm outer diameter, and 21 cm length. The UV irradiation source is a 125 W high pressure mercury vapor lamp (Samson, India). The outer glass shell was removed and placed inside the quartz tube for use. The ballast and capacitor were connected in series with the lamp to avoid fluctuations in the input power supply. Submersible water pump was used to circulate water through the jacket of the quartz tube to avoid heating caused by dissipative loss of UV light. The reactant solution along with the catalyst was taken in a beaker which was placed away from the quartz tube. The immobilized catalyst was placed in the solution, and the solution was stirred with magnetic stirrer to circulate the reactants over the catalyst continuously during the reaction. The whole reactor setup was enclosed in a wooden box.

Fabrication of PSS/TiO_2 Films. In the present study, thin films were immobilized using the LbL technique. To show the effectiveness of this method in terms of catalyst immobilization and photodegradation of the dye, it was compared with methods like drop casting and spin coating. For immobilizing the substrates using LbL technique, the glass slides were first cleaned by sonicating for 10 min in a solution containing 2:1(v/v) ratio of isopropanol and water. PSS and PAH each of concentration 1 g/L in DI water were prepared and adjusted to the desired pH. Water pH for rinsing purpose was adjusted to that of the polyelectrolytes. The multilayer thin films were deposited according to the method described previously by Decher and Hong (23). To deposit TiO_2 on glass substrates, a colloidal solution was made in DI water, and pH was adjusted such that it was stable during deposition and at the same time it had the desired charge to be suitable for LbL technique. Initially, one precursor monolayer of PAH was deposited to reverse the charge on the substrate, after which alternate layers of PSS/TiO_2 were assembled. The final layer was TiO_2 in all the cases. The notation for the polyelectrolyte and TiO_2 is subscript to the parentheses indicates the number of layers of the item

written in parentheses. For example, PAH/(PSS/TiO$_2$)$_5$ indicates that the first layer deposited is PAH and five alternate layers of PSS, and TiO$_2$. In all the catalyst immobilization experiments TiO$_2$, PAH, and PSS were deposited at pH 2.5. This pH was chosen based on the isoelectric point of colloidal TiO$_2$, which was found to be 6.6 (39). The TiO$_2$ particles are stable and positively charged below this isoelectric point and negatively charged above the isoelectric point. Since PSS is a strong polyelectrolyte it is negatively charged at all pH values and PAH which is a weak polyelectrolyte is strongly ionized at lower pH values (pH < 4) and positively charged at this pH (40).

The drop casting method (21) involves the preparation of a colloidal solution of TiO$_2$ that was evenly drop cast on top of the polymer and then dried on a hot plate or an oven at 50 °C. On the other hand, in the spin-coating method (22), the solid substrate is fixed on a spin coater and rotated at high speed (3000 rpm for 60 s in the present study) to spread the fluid by centrifugal force. Rotation is continued for some time, with fluid being spun off the edges of the substrate, until the desired film thickness is achieved. The catalysts were immobilized under the same process conditions that were used for dip LbL technique.

Photodegradation Experiments and Chemical Analysis. One hundred milliliters of the aqueous dye solution of desired concentration was taken in a beaker. The immobilized catalysts (of desired numbers and concentration) were placed vertically in the dye solution along the sides of the beaker. The solution was magnetically stirred in the dark for 30 min prior to irradiation to establish the adsorption−desorption equilibrium of the dye on the catalyst surface. The solution was stirred continuously and open to air during the reaction. The UV irradiation source was 10 cm apart from the reactant solution. The photodegradation of rhodamine B was determined at a wavelength of 553 nm. The samples were quantified by a standard calibration based on Beer−Lambert's law. At given irradiation time intervals, aliquots (2 mL) were taken from the solution, diluted to the required volume with DI water and analyzed by UV/vis spectrophotometer. All experiments were repeated for 2 times, and the variable range of data points was within ±5%. The degradation efficiency of rhodamine B was calculated as:

$$\eta\% = \frac{C_0 - C_t}{C_0} \times 100\%$$

where C_0 (mg/L) is original concentration of rhodamine B and C_t (mg/L) the concentration of rhodamine B at time t.

RESULTS AND DISCUSSION

Absorption Spectra of PAH/PSS/TiO$_2$ Thin Films. The absorption spectra of PELs (PAH and PSS), and TiO$_2$ was obtained using a UV/vis spectrophotometer. PELs of concentration 1 g/L each and TiO$_2$ concentration of 2 g/L (or 0.2 wt %) were prepared in DI water and deposited on glass slides. The deposition is done on both sides of the glass slides. So all absorbance plots correspond to the absorbance value of double the number of layers deposited. Initially, the absorbance spectrum was obtained for one bilayer of PAH, PSS, and TiO$_2$. The absorption spectra of PAH, PSS, and TiO$_2$ and their characteristic absorbance peaks show that TiO$_2$ has its maximum absorbance at ∼320 nm, that PSS shows maximum at ∼220 nm, and that PAH shows negligible absorbance in the UV−vis region. Hence the characterization for various samples was done in terms of TiO$_2$ or PSS absorbance.
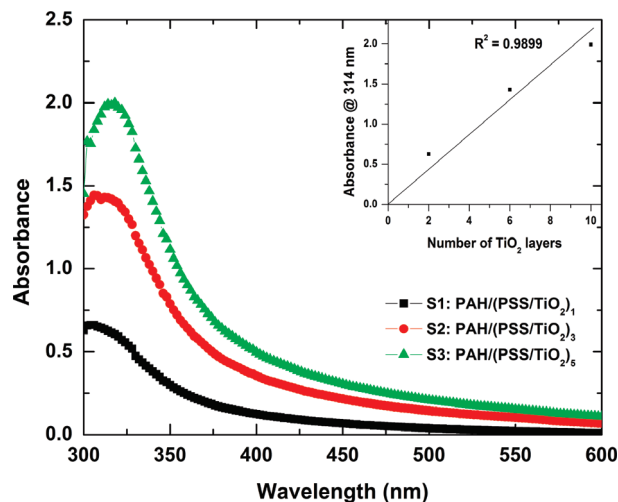

FIGURE 1. Absorption spectra of PAH, PSS, and TiO$_2$. Increase in absorbance with increase in number of TiO$_2$ layers (0.2 wt % TiO$_2$). Inset: Number of TiO$_2$ layers versus absorbance.

To ensure whether the polyelectrolytes are being deposited under the experimental conditions, different number of polyelectrolyte layers were prepared and deposited on glass slides. The absorbance spectra for each bilayer of deposition was obtained between 200 and 350 nm. The results showed that absorbance increases linearly with increasing number of polyelectrolyte layers (40). The absorbance basically corresponds to PSS since PAH does not show any absorbance above 190 nm. These results confirm the regular stepwise growth of the films.

In the next set of experiments, 1, 3, and 5 layers of TiO$_2$ were deposited on three glass substrates respectively with PAH as the initial layer above which alternative layers of PSS and TiO$_2$ were deposited. The PELs concentration is 1 g/L in DI water and that of TiO$_2$ is 0.2 wt %. The samples corresponding to 1, 3, and 5 layers of TiO$_2$ are named S1, S2, and S3, respectively. Absorption spectra were obtained for all the three samples between 300 and 600 nm as shown in Figure 1. Since glass absorbs light in the UV region and gives spurious peaks below 300 nm, this wavelength range has been chosen. Above 600 nm PAH, PSS and TiO$_2$ show negligible absorbance. The maximum absorption value (at 314 nm) in the spectrum corresponds to TiO$_2$ layer. The inset plot shows that absorption increases linearly with the number of TiO$_2$ layers indicating that the thickness of the individual TiO$_2$ layer is constant. Further, the effect of TiO$_2$ (0.4 wt %) concentration at the assembly stage for 1, 3, and 5 layers of TiO$_2$ deposited on glass substrates was done to increase TiO$_2$ loading on the substrate. The results showed that the absorbance is linear with increase in TiO$_2$ concentration.

Characterization Studies. The thickness of the multilayers deposited by LbL technique was measured using a noncontact optical profiling system. Experiments were carried out by increasing the PAH/(PSS/TiO$_2$)$_n$ bilayers from 1 to 20 using 0.4 wt % TiO$_2$ and PAH and PSS concentrations of 1 g/L each. Figure 2a shows the number of bilayers versus film thickness. The average thickness of each bilayer is estimated to be 19.5 nm. The thickness contributed per
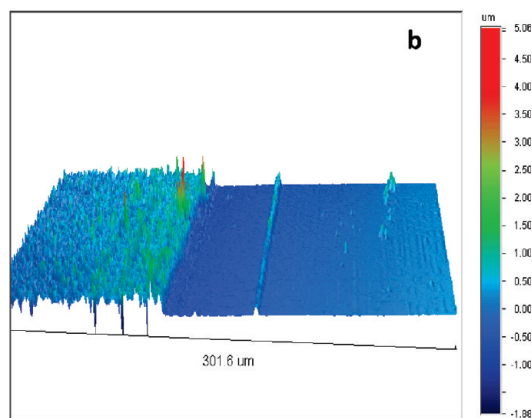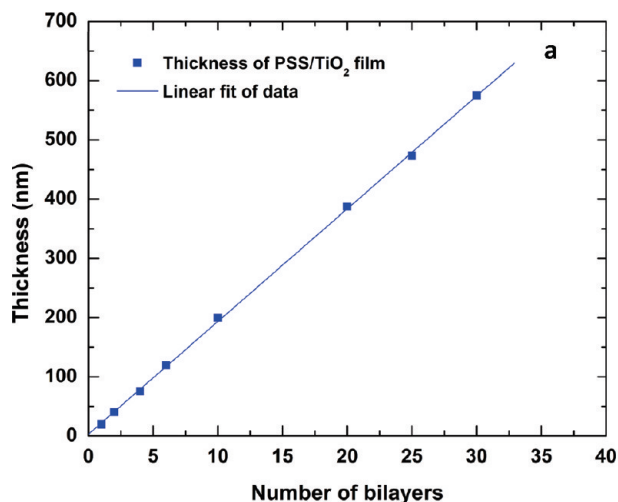
FIGURE 2. (a) Number of PAH/(PSS/TiO$_2$)$_n$ bilayers versus multilayer film thickness. (b) 3-D profile view of PAH/(PSS/TiO$_2$)$_{30}$.

FIGURE 3. AFM images of TiO$_2$ deposition on silicon wafers for PAH/ (PSS/TiO$_2$)$_1$ through (a) LbL route and (b) direct deposition.

bilayer for PSS, as determined by profilometry measurements, is ~0.5 nm. Since the average particle size of Degussa P25 is 21 nm, the thickness of one bilayer of PSS/TiO$_2$ film is estimated to be about 21.5 nm. Thus theoretically the total thickness of a PSS/TiO$_2$ film having 6 and 10 bilayers is expected to be 129 and 215 nm, respectively. The value obtained from profilometry was 120 and 200 nm. Also it can be observed that the film thickness increases linearly with increase in number of bilayers from 1 to 30 showing a uniform growth of the polyelectrolyte/TiO$_2$ films. The increase in thickness may also largely depend on the nature of the polyelectrolytes used, the pH at which they are deposited, and the average particle size of TiO$_2$ since this facilitates adsorbing more TiO$_2$ particles during the assembly process. In general, the bilayer thicknesses for the polycations like PDAC/TiO$_2$ and PAH/TiO$_2$ is estimated to be about 37 and 48 nm, respectively, per bilayer, whereas for the polyanions like PSS/TiO$_2$ and PAA/TiO$_2$ it is 18 and 19 nm per bilayer (41). Hence, the thickness found for PSS/TiO$_2$ per bilayer in the present study is agreement with these values. Figure 2b shows the 3-D profile view of a 30 bilayer PSS/TiO$_2$ film with thickness of 575 nm. The film shows an interface with coated (left) and uncoated (right) surfaces clearly depicting the uniform growth of the multilayer thin films.
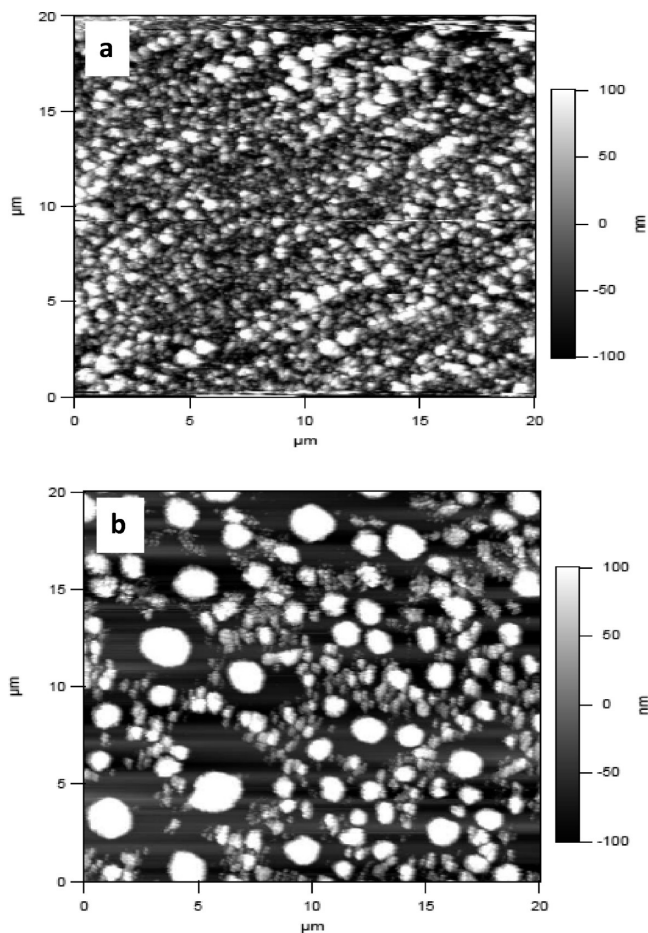
Further, the effectiveness of LbL method was verified using AFM by direct deposition of TiO$_2$, as well as by LbL techniques. TiO$_2$ concentration of 0.4 wt % was directly deposited on one slide without the deposition of polyelectrolytes, and on the other slide, PAH/(PSS/TiO$_2$)$_1$ films were deposited using 0.4 wt % TiO$_2$ and PAH, PSS concentrations of 1 g/L each by LbL method. The surface images for these samples are shown in Figure 3. The AFM images clearly indicate that LbL route yields better adsorption of particles and a better uniform surface when compared to direct deposition in which TiO$_2$ adsorbed as patches.

Characterization of the multilayer thin films was done using FEI-SEM to analyze and visualize the quality and morphology of the resulting film structures deposited by LbL technique. The ability of immobilized catalysts prepared by this technique was compared with TiO$_2$ films prepared by drop casting and spin coating methods. Figure 4 shows the SEM images of PAH/(PSS/TiO$_2$)$_6$ deposited with 0.4 wt % TiO$_2$ and PAH, PSS concentrations of 1 g/L each with all these techniques. It is very clear from these images that films prepared by drop-casting (Figure 4a) and spin-coating (Figure 4b) methods do not show uniform surface morphology when compared to LbL-TiO$_2$ films (Figure 4c) deposited under the same experimental conditions. It can also be seen that polyelectrolytes and TiO$_2$ are deposited as clusters in case of films assembled using drop casting and spin coating
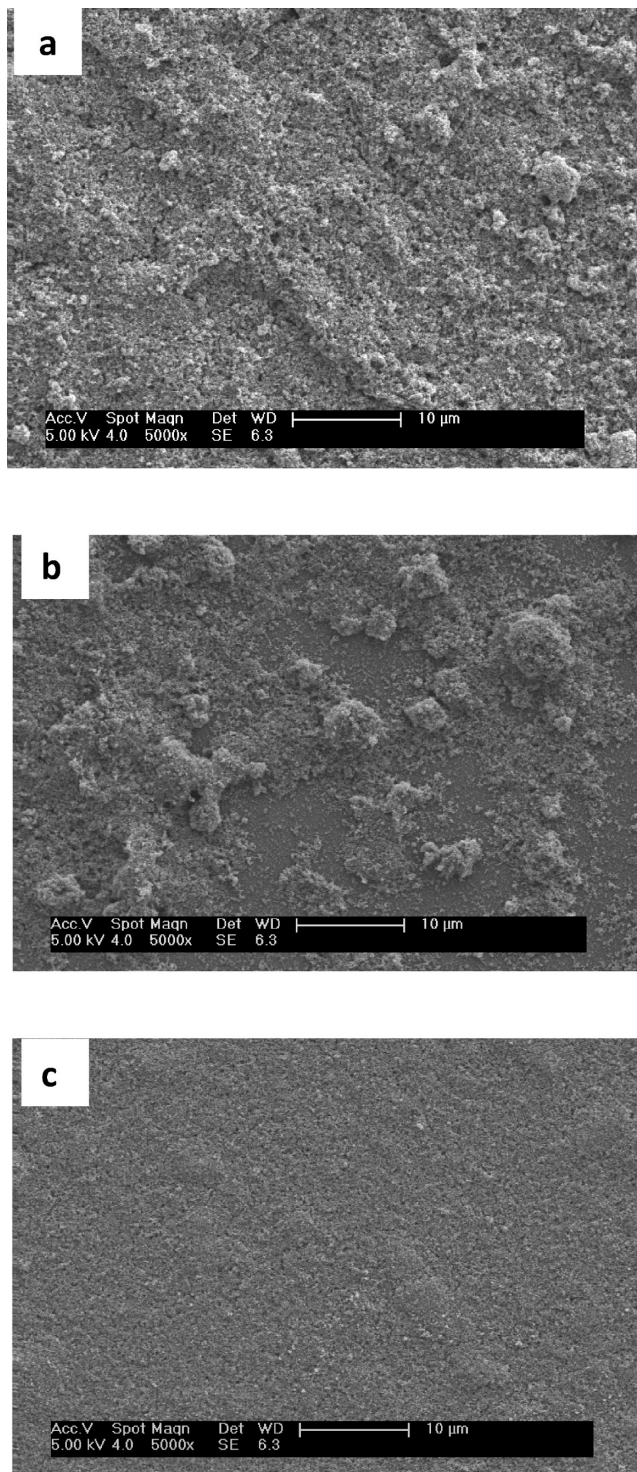
FIGURE 4. SEM images of PAH/(PSS/TiO$_2$)$_6$ immobilized catalysts at 5000 magnification deposited by (a) drop-casting, (b) spin-coating, and (c) LbL methods.

FIGURE 5. Degradation of rhodamine B under UV light in the presence of TiO$_2$ in suspension form. Initial dye concentration: 10 mg/L. Values in legend indicate the concentration of TiO$_2$.

the photocatalytic activity, as larger surface area provides for more photocatalysis reactions to take place.

This was also well demonstrated by Sohn et al. (34) showing that nanoparticles can have remarkably different photocatalytic properties because of their structural difference despite having the same internal sequence of polyelectrolytes and TiO$_2$ deposited by the dip SA and the spin SA methods. Therefore, in the present study comparison of the ability of catalysts prepared by different methods has been done in terms of photodegradation of rhodamine B.

Photodegradation Reactions. All photocatalytic degradation experiments were conducted with 100 mL of 10 mg/L rhodamine B, and the photoreactor setup is the same unless or otherwise mentioned. A control experiment was run for 9 h to see if there is any degradation of the dye when exposed to UV irradiation in the absence of catalyst. It was observed that there was hardly any degradation of the dye in the absence of the catalyst. To compare the efficiency of the immobilized catalysts with TiO$_2$ in suspension form, photodegradation experiments were initially conducted by varying TiO$_2$ concentrations from 0.005 to 1 g/L, and the results obtained are plotted in Figure 5. It is apparent that degradation is dependent on TiO$_2$ concentration, and complete degradation of the dye is obtained within 1 h with 1.0 g/L TiO$_2$ and 30−50 % in other cases under the same illumination time.

To check whether PSS will cause any degradation of rhodamine B, an experiment was carried out without any photocatalyst but in the presence of 100 mg/L PSS. The results indicate that there is no appreciable degradation of the dye for 5 h. Similarly another experiment was carried out with 100 mg/L PSS and 100 mg/L TiO$_2$ to see if PSS itself was getting degraded under UV irradiation. It was observed that that there is no appreciable degradation of PSS even after 90 min of irradiation showing that PSS is not degraded during the reaction.

Initially an experiment was performed with one immobilized catalyst, having one bilayer of PAH/(PSS/TiO$_2$)$_1$ prepared with 0.4 wt % TiO$_2$ and irradiated for 7 h. It was

methods. On the other hand, the SEM image of LbL-TiO$_2$ film illustrates a smooth surface morphology and a complex network of cross-linked polyelectrolytes with TiO$_2$ nanoparticles uniformly distributed in the multilayer thin films. It is also clear that with the amount of TiO$_2$ adsorbed, a dense layer had formed at the sixth bilayer. The image also shows a high degree of porosity, which plays an important role in
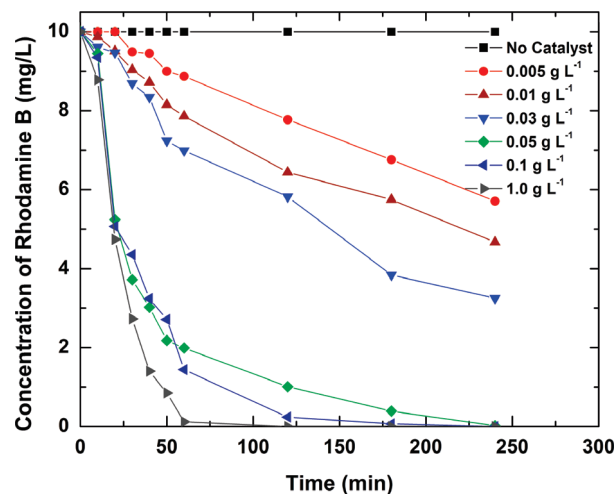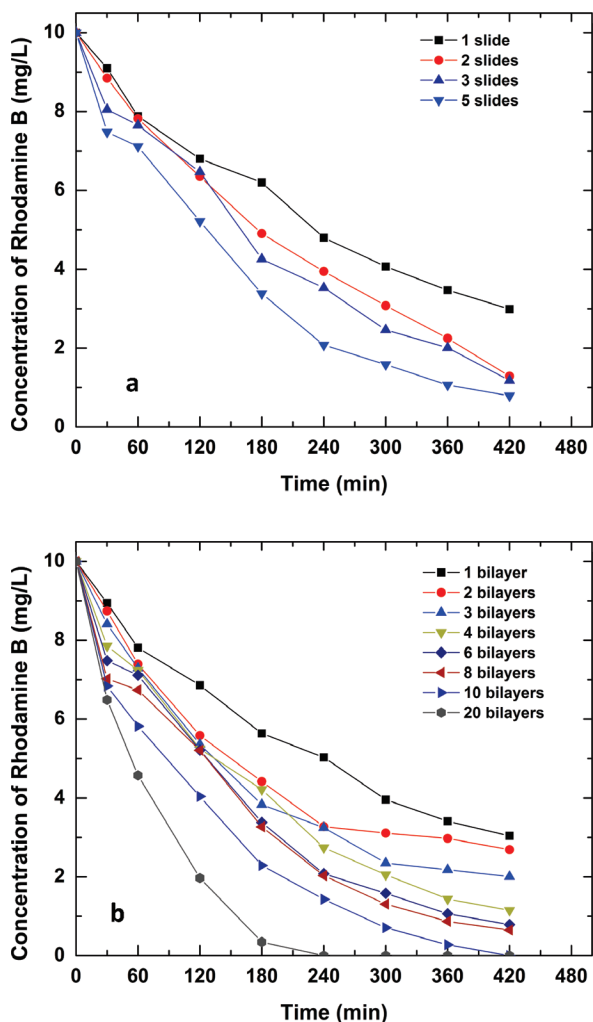
FIGURE 6. Photodegradation of rhodamine B under UV light by varying (a) number of catalysts and (b) number of bilayers. Initial dye concentration: 10 mg/L. Irradiation time: 420 min.

observed that percentage degradation increased with time and the concentration of the dye remaining in the solution at the end of seven hours was 2.9 mg/L, corresponding to a degradation efficiency of 70.1 %. Since the degradation was not complete under these process conditions experiments were performed by increasing the number of catalysts.

To study the effect of surface area on dye degradation, experiments were carried out for 7 h using 2, 3, and 5 immobilized catalysts instead of one prepared with 0.4 wt % TiO_2 and five bilayers of PAH/(PSS/TiO_2)$_5$. Figure 6a shows the results of this experiment. It can be observed that the degradation efficiency enhanced when more than one slide was used. The initial rate of degradation and degradation achieved after 7 h are summarized in Table 1. As the number of slides increased from 1 to 5, the initial rate of rhodamine B degradation also increased from 0.03 to 0.084 mg/L min^{-1}. The degradation efficiency also increased from 70.1 to 92 % in seven hours with 1 and 5 immobilized catalysts, respectively. The reason might be the availability of more catalyst surface area leading to better degradation efficiency. It should be pointed out that the increase in degradation rate is not linearly proportional to the increase in surface area. The photocatalytic activity of TiO_2 is determined not only

Table 1. Comparison of Initial and Final Conversion Rates for Different Operating Conditions

parameter	operating conditions	initial rate mg/L min^{-1}	% degradation after 7 h
TiO_2 in suspension	0.005 g/L	0	42.9[a]
	0.01 g/L	0.013	53.3[a]
	0.03 g/L	0.039	67.5[a]
	0.05 g/L	0.055	99.8[a]
	0.1 g/L	0.065	100[a]
	1.0 g/L	0.122	100[a]
effect of surface area	1 slide	0.030	70.1
	2 slides	0.038	87.1
	3 slides	0.064	88.2
	5 slides	0.084	92.0
effect of bilayers	1 bilayer	0.035	69.6
	2 bilayers	0.041	73.1
	3 bilayers	0.053	79.9
	4 bilayers	0.071	88.5
	6 bilayers	0.084	92.0
	8 bilayers	0.099	93.5
	10 bilayers	0.105	100
	20 bilayers	0.117	100[a]
effect of initial dye concentration	5 mg/L	0.019	100
	10 mg/L	0.069	100
	25 mg/L	0.037	74.4
	50 mg/L	0.028	43.5

[a] Conversion after 4 h.

by the available surface area of the catalyst but also by the incident UV light intensity and slide orientation. It should be pointed out that the incident light intensity in all these experiments was same. Furthermore, all the slides may not be oriented in an identical manner, and thereby, the absorption of UV light and generation of radicals may not be same for all the slides.

Figure 6b shows the effect of number of bilayers on dye degradation. This was done by varying the bilayers from 1 to 20 (TiO_2 = 0.4 wt %; number of immobilized catalysts = 5; irradiation time = 7 h). The graph depicts that degradation efficiency increases with increase in number of bilayers. The initial rate and degradation efficiency after 7 h is summarized in Table 1. The efficiency increased from 69.6 % to 100 % with 1 and 10 bilayers respectively in seven hours and in case of catalysts with 20 bilayers, the degradation was 100 % in four hours. Table 1 clearly shows that the initial rate of degradation increases as the number of bilayers increases. This observation clearly points to the fact that the degradation is not only carried out by TiO_2 on the uppermost layer (surface layer) but the inner layers also contribute to the dye degradation. However, the increase in degradation rate is not linear with increase in number of bilayers. This observation implies that the efficacy of TiO_2 in the inner layers is not same as that in the uppermost layer. As the number of layers increase, the diffusion of the dye as well as reactive species in- and out of the layers also plays an important role in determining the degradation kinetics. These results clearly show that more TiO_2 is getting immobilized on the multilayers which in turn increase the
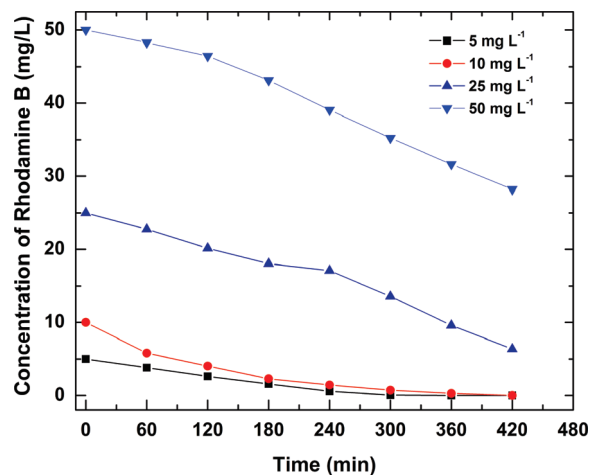
FIGURE 7. Effect of initial dye concentration on its photodegradation. The values in the legend indicate the initial concentration of the dye. Irradiation time: 420 min.
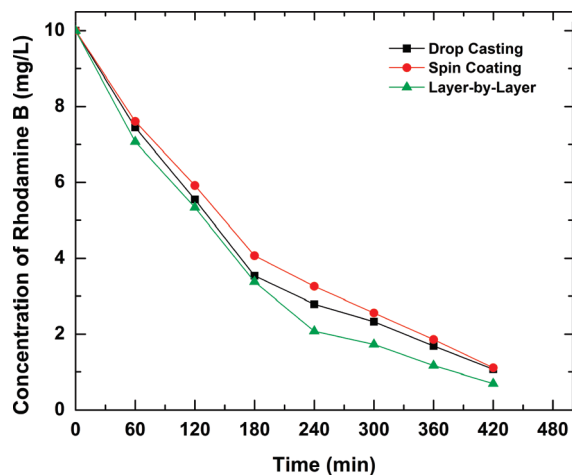

FIGURE 8. Comparison of photodegradation of rhodamine B under UV light by drop-casting, spin-coating, and layer-by-layer methods. Initial dye concentration: 10 mg/L. Irradiation time: 420 min.

degradation kinetics. The suitable surface structure and porosity increases the photocatalytic activity and in turn degradation efficiency. This is evident from the SEM images (Figure 4c) of the films showing uniformly distributed TiO_2 in different bilayers indicating that the growth of the films is regular. When TiO_2 is used in suspension form, 100 % degradation efficiency is achieved within 60 min. But the major drawback is the difficulty in separating the nano-TiO_2 from the clean water. On the other hand, 100 % degradation of the dye is achieved in 240 min with TiO_2 immobilized slides deposited using TiO_2 concentration of 0.4 wt %. However, the solution is clean and free of any suspended nanoparticles, which can be safely discharged to the environment. This advantage of process simplification overrides the disadvantage of slower kinetics with immobilized catalyst and makes it an attractive option for field work.

To check whether the polyelectrolyte layers are obstructing the adsorption of reactant by the inner catalyst layers, PSS and PSS/PAH were deposited as the top layer on PAH/(PSS/TiO_2)$_5$ sample. The results indicate that there is no appreciable change in the degradation of rhodamine B with PAH/(PSS/TiO_2)$_5$, PAH/(PSS/TiO_2)$_5$ + PSS, and PAH/(PSS/TiO_2)$_5$ + PSS + PAH, which is ~70 % in all the cases in seven hours.

Effect of Initial Dye Concentration. Figure 7 shows the effect of initial Rhodamine B concentration on its photodegradation. This was studied by varying the dye concentration from 5 − 50 mg/L (TiO_2 = 0.4 wt %; PAH/(PSS/TiO_2)$_{10}$; number of immobilized catalysts = 5; irradiation time = 7 h). The results obtained are compared with dye concentration of 10 mg/L under the same set of experimental conditions. It can be observed that as the concentration of rhodamine B increases, the percentage degradation decreases from 100 % to 74.48 % and to 43.58 % for 10 mg/L, 25 mg/L and 50 mg/L respectively in seven hours (Table 1). The decrease in degradation rates with increasing dye concentration can be explained based on two reasons: (1) the light intensity reaching the TiO_2 film surface is reduced because of the lower transparency of the solution at higher dye concentrations (10, 36), and (2) since the illumination
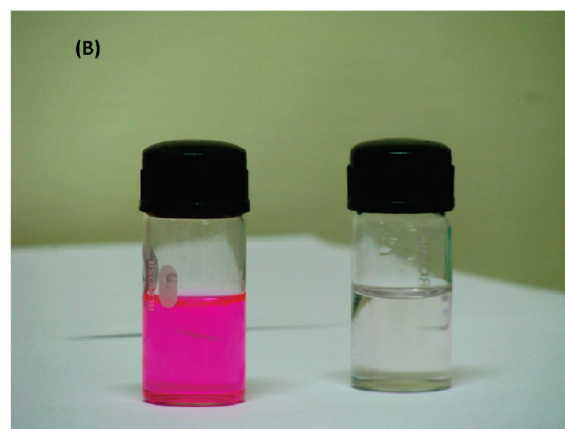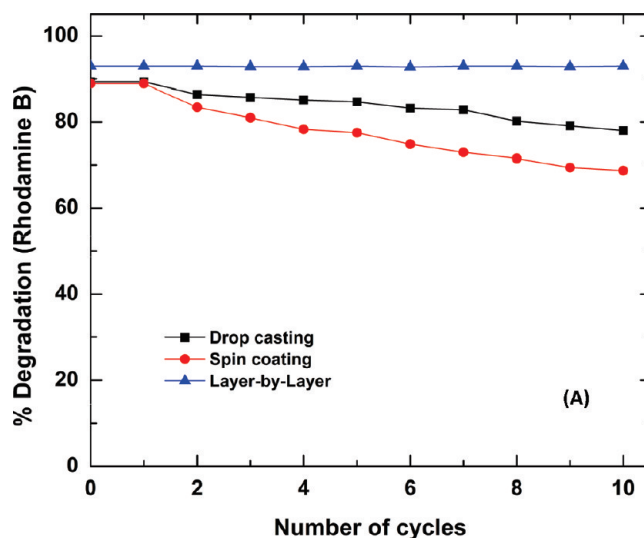
FIGURE 9. (A) Number of cycles versus percentage degradation of rhodamine B using catalysts prepared by drop-casting, spin-coating, and layer-by-layer methods. (B) Pictorial representation of photodegradation of rhodamine B dye (a) at the start of first cycle and (b) after ten cycles using catalysts prepared by LbL technique.

time and light intensity are constant and as more and more organic substances are adsorbed on to the surface of TiO_2 at higher concentrations, the free radicals formed on the
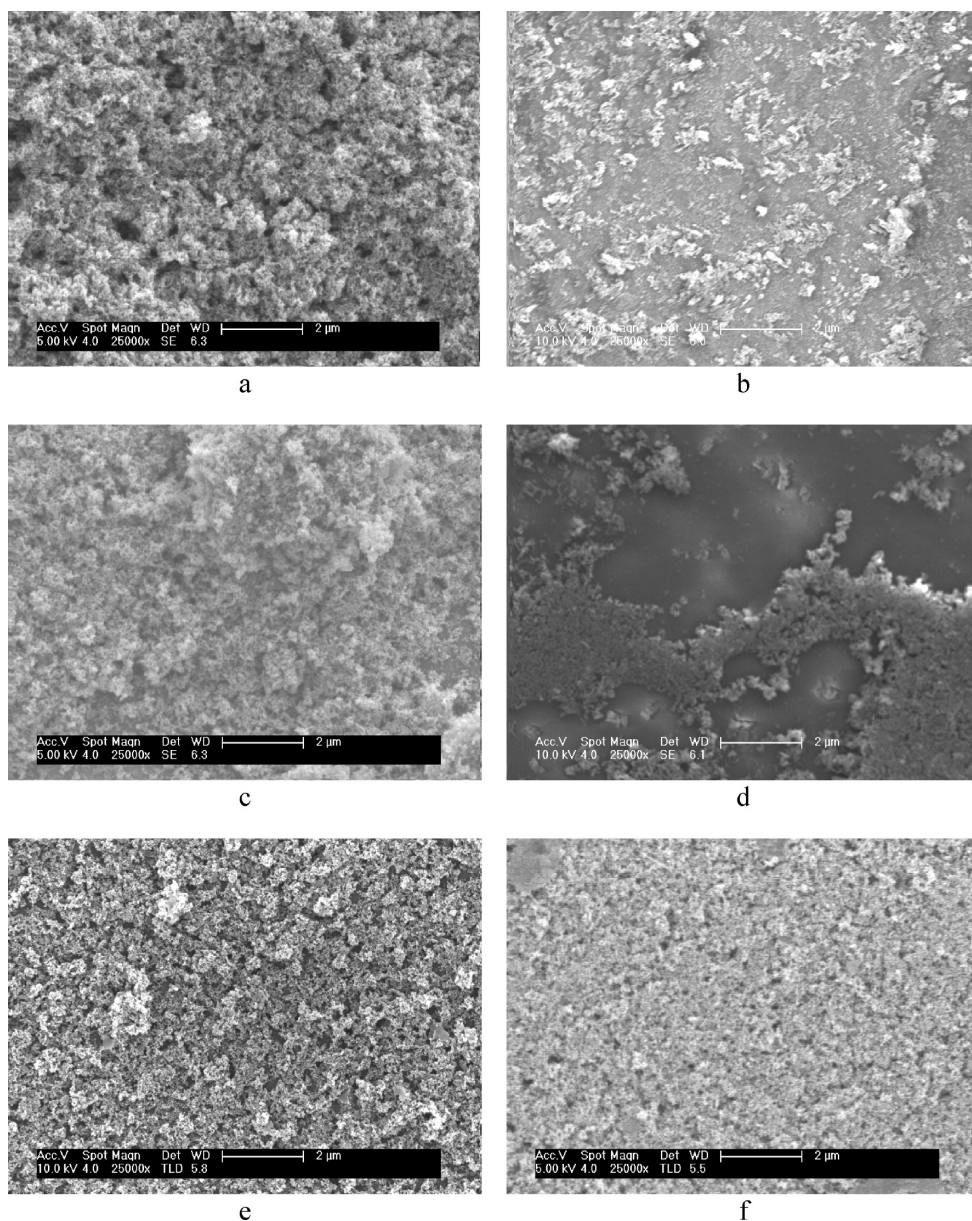
Priya et al.

FIGURE 10. SEM images of PAH/(PSS/TiO₂)₆ immobilized catalysts before (a, c, e) and after ten cycles (b, d, f) of photodegradation. Catalysts were prepared using drop-casting (a, b), spin-coating (c, d), and layer-by-layer methods (e, f).

surface of TiO₂ also remain constant in turn decreasing the oxidation of the dye and its products formed. However the results clearly demonstrate that the method could be successfully applied to degrade dye concentrations ≤25 mg/L.

Catalyst Reusability. Catalyst reusability studies are very important in terms of cost considerations because this can reduce the cost on input materials. These studies were performed with catalysts immobilized using drop casting, spin coating and LbL methods for 10 cycles to see the efficiency in degrading the dye. Experiments were conducted under the following process conditions: $TiO_2 = 0.4$ wt %, $PAH/(PSS/TiO_2)_6$, immobilized catalysts = 5, dye concentration = 10 mg/L, irradiation time = 7 h. To compare the efficiency, after the first cycle of reaction, the degraded dye solution was removed and a fresh solution (10 mg/L) of the dye was placed in the beaker without removing the

catalysts. The same procedure was repeated for nine more cycles. Samples were collected at the end of each cycle and analyzed to see the percentage degradation of the dye in seven hours. Figure 8 shows the results of first cycle of rhodamine B with TiO₂ immobilized with three different techniques. It can be seen that the performance of LbL technique is similar to that of drop casting and spin coating techniques. However, the superiority of LbL technique over other two methods in synthesis of stable film is apparent with repeated use of the immobilized catalyst. Figure 9a shows the number of cycles versus percentage degradation of rhodamine B at each cycle using all the three methods. It was observed that the catalysts prepared with the other two methods showed a gradual decrease in the dye degradation efficiency from 89.3 % to 78 % and 88.9 % to 68.7 % for drop-casting and spin-coating methods respectively at the end of tenth cycle. On the other hand, with the

ACS APPLIED MATERIALS & INTERFACES

catalysts prepared by LbL method, each experiment included 93% degradation efficiency of the dye at 7 h and perfectly reproduced the same results at the end of each cycle. An experiment conducted with PAH/(PSS/TiO$_2$)$_{10}$ film yielded similar type of results indicating 100% dye degradation efficiency in 7 h and catalyst reusability for several cycles. The pictorial representation of this experiment, that is, the dye at the start of the first cycle and after ten cycles of photodegradation is shown in Figure 9b. The results indicate that the catalyst prepared using LbL method did not lose its photocatalytic activity even after several repeated uses. These results were confirmed with SEM images also (Figure 10). From the images it is apparent that catalysts prepared using the other two methods showed a loss of the multilayers after repeated uses in turn lowering the dye degradation efficiency. On the other hand, no alteration in the surface characteristics of TiO$_2$ on the LbL-TiO$_2$ thin films was observed indicating its stability after several cycles of operation. Moreover no erosion of TiO$_2$ has taken place making this technique a very robust one for field work.

Catalyst Loading. The amount of catalyst deposited per each slide was determined by calculating the difference between the weight of the empty slide and the weight after 10 bilayers of TiO$_2$ deposition. Also, the weight after each layer of TiO$_2$ deposition (excluding the weight of PSS layer) was determined. On an average, the amount of TiO$_2$ deposited per each slide, was ∼3.69 mg, and the average deposition per each layer is ∼0.33 mg. For example, the amount of TiO$_2$ required for the preparation of catalyst with 10 bilayers and 5 slides to degrade 100 mL of 10 mg/L dye is approximately 18.45 mg, which would be sufficient to completely degrade the dye. The immobilized catalyst can also be reused several times. The amount of catalyst required when TiO$_2$ was used in suspension form for the complete degradation of 100 mL of the dye is 100 mg, which is very high as compared to TiO$_2$ loading on the slides using LbL technique.

Degradation Kinetics. Photocatalytic degradation of various dyes over illuminated TiO$_2$ can be fitted by the Langmuir−Hinshelwood (L−H) kinetics model (42)

$$\Gamma = -\frac{\mathrm{d}C}{\mathrm{d}t} = \frac{\mathscr{K}KC}{1 + KC} \tag{1}$$

Where Γ is the oxidation rate of the reactant (mg/L min), C is the concentration of the reactant (mg/L), t the illumination time, $\mathscr{K}$ the reaction rate constant (mg/L min), and K is the adsorption coefficient of the reactant (L/mg). When the chemical concentration C_0 is small ($KC_0 \ll 1$), the above equation can be simplified to an apparent first-order equation

$$\ln \frac{C}{C_0} = -K_{\mathrm{app}}t \tag{2}$$

A plot of $\ln(C/C_0)$ versus time represents a straight line, the slope of which upon linear regression equals the appar-

Table 2. Values of k_{app} and Regression Coefficient (R^2) for Degradation Studies Carried out under Different Operating Conditions

parameter	operating conditions	$-K_{\mathrm{app}}$	R^2
TiO$_2$ in suspension			
	0.005 g/L	0.14	0.994
	0.01 g/L	0.19	0.987
	0.03 g/L	0.29	0.983
	0.05 g/L	1.34	0.938
	0.1 g/L	1.39	0.943
	1.0 g/L	4.1	0.913
effect of surface area			
	1 slide	0.17	0.994
	2 slides	0.27	0.978
	3 slides	0.28	0.985
	5 slides	0.36	0.995
effect of bilayers			
	1 bilayer	0.17	0.994
	2 bilayers	0.19	0.937
	3 bilayers	0.24	0.970
	4 bilayers	0.31	0.996
	6 bilayers	0.36	0.995
	8 bilayers	0.39	0.992
	10 bilayers	0.96	0.73
	20 bilayers	1.61	0.877

ent first-order rate constant k_{app}. Table 2 shows the values of k_{app} and regression coefficient (R^2) for degradation studies carried out under different operating conditions. It can be seen from Table 2 that the R^2 values for most of the cases are close to unity indicating that the first order decay kinetics adequately explains the experimental results. It should be pointed out that the increase in number of slides from 1 to 5 leads to increase in surface area, and therefore, k_{app} also increases. However, the increase in k_{app} is not proportional to the increase in surface area. This may be attributed to the positioning of the multiple slides in the reactor along the circumference of the reactor. As a result the incident UV light intensity is not exactly identical for all the slides. Increasing the number of bilayers on a single slide also leads to increase in the value of k_{app}. However, the regression fit is rather poor for 10 and 20 bilayers which indicate the deviation from first-order kinetics. This can be attributed to the increasing diffusional resistances and, therefore, accessibility of catalyst located in the inner layers.

CONCLUSIONS

TiO$_2$ multilayer thin films were fabricated using the LbL technique. A pH of 2.5 was chosen to deposit the polyelectrolytes and TiO$_2$. The process conditions for the complete degradation of 100 mL of the dye containing 10 mg/L were 5 immobilized catalyst slides having 20 bilayers of polyelectrolyte/TiO$_2$ under UV irradiation time of 4 h. Comparison of LbL method with other methods, such as drop-casting and spin-coating techniques, was done to prove its efficiency in degrading the dye. Though these methods are not time-consuming, the superiority of LbL technique over other two methods in terms of film stability and catalyst reusability has

been highlighted. The main advantage of this technique is its applicability to any kind of shape and substrate, which makes an attractive option for scaleup. Though the illumination time is longer when compared to that used in suspension form, it is apparent that the reaction time can be reduced with increase in number of bilayers. Also, the amount of TiO_2 required to completely degrade the dye by LbL technique is much less than that required for TiO_2 in suspension form. The methodology employed, overcomes all the problems associated with the use of TiO_2 powders reported earlier. Since the catalyst can be reused several times with the same efficiency, this method can be successfully applied to continuous systems with significant savings in terms of TiO_2 and polymer requirement. This is very important in terms of overall cost of treating water. The results obtained suggest that this approach is a promising alternative to the existing methods for the treatment of textile industry waste waters. This methodology can also be applied for the degradation of other organics in wastewaters.

REFERENCES AND NOTES

(1) Chen, X.; Mao, S. S. *Chem. Rev.* **2007**, *107*, 2891.
(2) Soares, E. T.; Lansarin, M A.; Moro, C. C. *Braz. J. Chem. Eng.* **2007**, *24*, 29.
(3) Yu, D.; Cai, R.; Liu, Z. *Spectrochim. Acta, Part A* **2004**, *60*, 1617.
(4) Karunakaran, C.; Senthilvelan, S. *Electrochem. Commun.* **2006**, *8*, 95.
(5) Kapinus, E. I.; Viktorova, T. I.; Khalyavka, T. A. *Theor. Exp. Chem.* **2006**, *42*, 282.
(6) Martnez, C. L. T.; Kho, R.; Mian, O. I.; Mehra, R. K. *J. Colloid Interface Sci.* **2001**, *240*, 525.
(7) Liao, D. L.; Liao, B. Q. *J. Photochem. Photobiol., A* **2007**, *187*, 363.
(8) Priya, M. H.; Madras, G. *J. Photochem. Photobiol., A* **2006**, *178*, 1.
(9) Sivalingam, G.; Nagaveni, K.; Hegde, M. S.; Madras, G. *Appl. Catal., B* **2003**, *45*, 23.
(10) Daneshvar, N.; Salari, D.; Khataee, A. R. *J. Photochem. Photobiol. A* **2003**, *157*, 111.
(11) Amrit Pal, T.; Anoop, V.; Jotshi, C. K.; Bajpai, P. K.; Vasundhara, S. *Dyes Pigm.* **2006**, *68*, 53.
(12) Zhang, F.; Zhao, J.; Zang, L.; Shen, T.; Hidaka, H.; Pelizzetti, E.; Serpone, N. *J. Mol. Catal. A: Chem.* **1997**, *120*, 173.
(13) Li, J.; Ma, W.; Chen, C.; Zhao, J.; Zhu, H.; Gao, X. *J. Mol. Catal A: Chem.* **2007**, *261*, 131.
(14) Andronic, L.; Duta, A. *Thin Solid Films* **2007**, *515*, 6294.
(15) Ma, Y.; Yao, J. *J. Photochem. Photobiol., A* **1998**, *116*, 167.
(16) Takeuchi, M.; Itoh, T.; Nagasaka, H. *Thin Solid Films* **1978**, *51*, 83.
(17) Yeung, K. S.; Lam, Y. W. *Thin Solid Films* **1983**, *109*, 169.
(18) Yamashita, H.; Nakao, H.; Takeuchi, M.; Nakatani, Y.; Anpo, M. *Nucl. Instr. Methods Phys. Res., Sect. B* **2003**, *206*, 898.
(19) Chang, J. T.; Su, C. W.; He, J. L. *Surf. Coat. Technol.* **2006**, *200*, 3027.
(20) Negishi, N.; Takeuchi, K.; Ibusuki, T. *J. Sol−Gel Sci. Technol.* **1998**, *13*, 691.
(21) Qiao, Q.; Xie, Y.; Mc Leskey James, T. *J. Phys. Chem. C* **2008**, *112*, 9912.
(22) Song, S.; Liu, H.; Guo, X.; Hu, N. *Electrochim. Acta* **2009**, *54*, 5851.
(23) Decher, G.; Hong, J. D. *Ber. Bunsen Phys. Chem.* **1991**, *95*, 1430.
(24) Schmitt, J.; Decher, G.; Dressick, W. J.; Brandow, S. L.; Geer, R. E.; Shashidhar, R.; Calvert, J. M. *Adv. Mater.* **1997**, *9*, 61.
(25) Fendler, J. H. *Chem. Mater.* **1996**, *8*, 1616.
(26) He, J. A.; Mosurkal, R.; Samuelson, L. A.; Li, L.; Kumar, J. *Langmuir* **2003**, *19*, 2169.
(27) Kniprath, R.; Duhm, S.; Glowatzki, H.; Koch, N.; Rogaschewski, S.; Rabe, J. P.; Kirstein, S. *Langmuir* **2007**, *23*, 9860.
(28) Hattori, H. *Adv. Mater.* **2001**, *13*, 51.
(29) Lee, S. H.; Kumar, J.; Tripathy, S. K. *Langmuir* **2000**, *16*, 10482.
(30) Bhadra, D.; Gupta, G.; Bhadra, S.; Uma Maheshwari, R.; Jain, N. *J. Pharm. Pharm. Sci.* **2004**, *7*, 241.
(31) Lvov, Y.; Ariga, K.; Onda, M.; Ichinose, I.; Kunitake, T. *Langmuir* **1997**, *13*, 6195.
(32) Naskar, S.; Pillay, S. A.; Chanda, M. *J. Photochem. Photobiol., A* **1998**, *113*, 257.
(33) Kim, T. H.; Sohn, B. H. *Appl. Surf. Sci.* **2002**, *201*, 109.
(34) Sohn, B. H.; Kim, T. H.; Char, K. *Langmuir* **2002**, *18*, 7770.
(35) Wu, J. M.; Zhang, T. W. *J. Photochem. Photobiol., A* **2004**, *162*, 171.
(36) Zhang, L.; Zhu, Y.; He, Y.; Li, W.; Sun, H. *Appl. Catal., B* **2003**, *40*, 287.
(37) Kim, D. S.; Park, Y. S. *Chem. Eng. J.* **2006**, *116*, 133.
(38) Li, J.; Li, L.; Zheng, L.; Xian, Y.; Jin, L. *Electrochim. Acta* **2006**, *51*, 4942.
(39) Yu, H. H.; Jiang, D. S.; Li, X. F.; Yu, D. S.; Zhou, L. D. *Opt. Mater.* **2007**, *28*, 1381.
(40) Decher, G. In *Multilayer Thin Films, Polyelectrolyte Multilayers an Overview*; Decher, G., Schlenoff, J. B., Eds.; Wiley-VCH: Weinheim, Germany, 2003; p 3.
(41) He, J.; Ravi, M.; Samuelson, L. A.; Li, L.; Jayant, K. *Langmuir* **2003**, *19*, 2169.
(42) Hoffmann, M. R.; Martin, S. T.; Choi, W.; Bahnemann, D. W. *Chem. Rev.* **1995**, 95.

AM900566N